Director field and lifetime of the cholesteric storage mode

Marshall Luban
Department of Physics, Bar-Ilan University, Ramat-Gan, Israel
and Department of Electronics, Weizmann Institute of Science, Rehovot, Israel

Shmuel Shtrikman*
Department of Electronics, Weizmann Institute of Science, Rehovot, Israel

Joel Isaacson†
Department of Physics, Bar-Ilan University, Ramat-Gan, Israel
(Received 22 May 1975; revised manuscript received 3 September 1976)

The detailed spatial dependence of the director field $\vec{n}(\vec{r})$ for the metastable cholesteric storage mode is calculated as a function of plate spacing and surface energy coefficient. These calculations are first performed subject to the constraint that $\vec{n}$ is confined to a plane perpendicular to the plates. Upon waiving the planarity constraint and solving the complete Euler-Lagrange equations, we find that the departure of $\vec{n}$ from the plane is less than 7°, with the largest values occurring in the immediate vicinity of the plates. Employing our results for $\vec{n}(\vec{r})$, we calculate the dependence of the electrical capacitance on plate spacing. We also propose a mechanism for the decay of the storage mode as well as a simple semiphenomenological expression for its lifetime. For a suitable choice of parameters our theoretical expressions are in reasonably good agreement with the capacitance and lifetime measurements of Hulin for variable plate spacing.

I. INTRODUCTION

The experimental observation of a long-lived metastable mode in cholesteric liquid crystals has attracted considerable interest in the past few years.[1-12] This mode[13] is thought to be a configuration where the axis of the helical ordering lies parallel to the plates-cholesteric sandwich, in contrast to the more familiar, stable (Grandjean) mode where the axis is perpendicular to the plates.

Recently, a theoretical model of the metastable mode was presented,[12] according to which the cholesteric helix unwinds continuously, starting from the pitch $2\lambda_0$ of the bulk cholesteric, to the nematic configuration, as the plate spacing $2L$ is decreased to a critical value $2L_c$. This model is based on the following picture. The surface interaction between the cholesteric and the treated confining plates, characterized by a surface-energy coefficient C, is such as to constrain the director at the plates to lie exclusively in a plane (xy) and to favor alignment in the y direction (see Fig. 1). It is then assumed that throughout the cholesteric sandwich the director lies in the xy plane and that it can be written as $\vec{n}(\vec{r}) = \hat{x}\sin\Phi(x,z) + \hat{y}\cos\Phi(x,z)$. The equilibrium director angle $\bar{\Phi}(x,z;L,C)$ was found by minimizing the total free functional for given values of L and C. Specifically, the total free energy is chosen as the sum of the usual Frank free-energy expression for a (left-handed) cholesteric[14] and a surface free energy (per unit volume) of the form

$$(2L\lambda)^{-1}\int_{-L}^{L}dx\int_{-\lambda/2}^{\lambda/2}dz\left[\tfrac{1}{2}Cf(\Phi)\right]\left[\delta(x-L)+\delta(x+L)\right],$$

where $f(\Phi)=\Phi^2$, $-\frac{1}{2}\pi<\Phi<\frac{1}{2}\pi$, and $f(\Phi+\pi)=f(\Phi)$, and 2λ is the assumed pitch of the cholesteric. The resulting Euler-Lagrange equation is solved subject to the symmetry properties[15] $\Phi(x,-z) = -\Phi(x,z)$, $\Phi(-x,z)=\Phi(x,z)$, and the boundary conditions $\Phi(x,z+\lambda)=\pi+\Phi(x,z)$, $\partial\Phi(\pm L,z)/\partial z = \mp(C/K)\Phi(\pm L,z)$. The equilibrium pitch, denoted

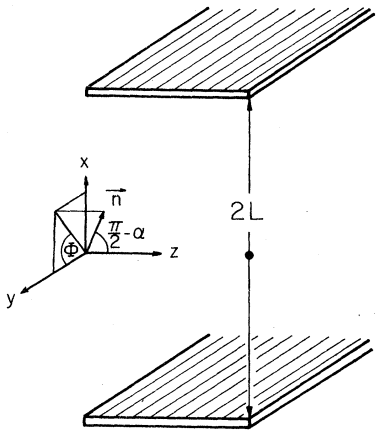

FIG. 1. Schematic diagram of the geometry of the two parallel infinite plates separated by a distance $2L$. The orientation of the director $\vec{n}$ can be specified by the angles α and Φ.

by $2\bar{\lambda}(L,C)$, and director angle $\bar{\Phi}$, are those values of 2λ and Φ which correspond to the absolute minimum of the total free energy for a planar director. The dependence of $\bar{\lambda}$ on L and C was given in Ref. 12, whereas the result for $\Phi(x,z)$ was left as a complicated infinite series in the variables x and z. In Sec. II we establish the detailed spatial dependence of the director angle Φ. For several special cases our results are given in closed analytic form, whereas more generally these are given in numerical form.

In Sec. III we waive the assumption of a planar director and solve the exact Euler-Lagrange equations which minimize the total free energy with respect to *all* spatial variations of $\vec{n}$. Specifically, we consider the case where the surface interaction gives rise to strong anchoring ($\vec{n}$ parallel to the y axis) on the plate faces. We find that the director is very nearly confined to the xy plane. The maximum departure of $\vec{n}$ from the xy plane occurs in the immediate vicinity of the plates and it is approximately 7°. These results would warrant adopting the mathematically simplifying assumption of a planar director field, as suggested in Ref. 12.

In Sec. IV, the results obtained in Sec. II are used to calculate the dependence of the electrical capacitance on plate spacing, and we compare our theoretical results with existing experimental data. In Sec. V we propose a mechanism for the decay of the metastable mode as well as a simple, semiphenomenological expression for the lifetime of the mode as a function of plate spacing. The free parameters in the lifetime expressions are determined by a best fit to lifetime data. We conclude with a discussion and summary in Sec. VI.

II. PLANAR DIRECTOR FIELD

As stated in Sec. I, the theoretical model of the storage mode of Ref. 12 is based on the simplified description, whereby the director field is planar-like, of the form $\vec{n}(\vec{r}) = \hat{x}\sin\Phi(x,z) + \hat{y}\cos\Phi(x,z)$. In this section we determine the detailed spatial dependence of the director angle $\Phi(x,z)$ for a variety of cases.

It was shown in Ref. 12 that the total free-energy functional has a *local* minimum if Φ is given by[14]

$$\Phi(x,z;\mathfrak{C}) = qz + \sum_{n=1}^{\infty} \frac{(-1)^n}{n} \times [n\mathfrak{C}^{-1}\sinh(2nqL) + \cosh(2nqL)]^{-1} \times \cosh(2nqx)\sin(2nqz), \qquad (2.1)$$

where $2L$ is the plate spacing, $\mathfrak{C} = C(2Kq)^{-1}$, $q = \pi/\lambda$, and the pitch 2λ is arbitrary. As stated in Sec. I, the equilibrium pitch, $2\bar{\lambda}(L,C)$, and director angle $\bar{\Phi}$, are those values of 2λ and Φ which correspond to the *absolute* minimum of the free energy for a planar director. The dependence of $\bar{\lambda}$ on L and C has been studied in detail in Ref. 12. For our present purposes it suffices to remark, first, that $\bar{\lambda}(L\to\infty,\mathfrak{C}) = \lambda_0$, where $2\lambda_0$ denotes the equilibrium pitch of the bulk cholesteric, and, second, $\bar{\lambda}$ increases continuously with decreasing L and diverges when $L = L_c$, where the critical spacing L_c is a function of the parameter $\lambda_0 C/K_1$.[16] The expressions for Φ given below apply for arbitrary pitch 2λ, but it shall be understood that λ is to be identified with $\bar{\lambda}$. We will investigate the behavior of Φ as one considers plate spacings decreasing from infinity ($\lambda = \lambda_0$) towards the critical spacing $2L_c$ ($\lambda\to\infty$). There are two important, distinct regimes: $L/\lambda \gtrsim 1$ and $L/\lambda \lesssim 1$. We begin by considering the regime $L \gtrsim \lambda$.

Consider first the case $\mathfrak{C} = \infty$, corresponding to the molecules at the plate faces being anchored parallel to the y axis. As long as $L \geq \lambda$ it is an excellent approximation, for all n, to replace $\cosh(2\pi nL/\lambda)$ by $\frac{1}{2}e^{(2\pi nL/\lambda)}$, and then, as shown in Appendix B, the series in Eq. (2.1) can be summed to give

$$\Phi(x,z;\infty) = -qz + \tan^{-1}[\tan(qz)\tanh q(L-x)] + \tan^{-1}[\tan(qz)\tanh q(L+x)]. \qquad (2.2)$$

In fact, if $L \geq 2\lambda$, the first and third (second) terms of Eq. (2.2) essentially cancel each other if $x > 0$ (<0) and thus Φ is well approximated by the simpler expression[17]

$$\Phi(x,z;\infty) \simeq \tan^{-1}[\tan(qz)\tanh q(L-|x|)]. \qquad (2.3)$$

In Fig. 2 we have plotted Φ, as given by Eq. (2.3), as a function of z in the range $0 \leq z \leq \frac{1}{2}\lambda$ and for several values of x in the close proximity of the upper plate at $x = L$. A striking feature of these curves is that at distances greater than approximately 0.2λ from the plate face, the director angle is already well approximated by the expression $\Phi = \pi z/\lambda$, which applies for bulk cholesteric. For a fixed value of x, in the immediate vicinity of the plate face, as z increases from zero, the director angle remains extremely small due to the strong anchoring boundary condition which applies for the present case of $\mathfrak{C} = \infty$. However, as z is increased towards $\frac{1}{2}\lambda$, the director angle rises steeply, passes through the value $\frac{1}{2}\pi$ at $z = \frac{1}{2}\lambda$ and reaches a value slightly less than π for z just beyond $\frac{1}{2}\lambda$. In this fashion one meets the requirement that, for all x, Φ must increase by π as z increases by λ.

We now consider the behavior of Φ for finite

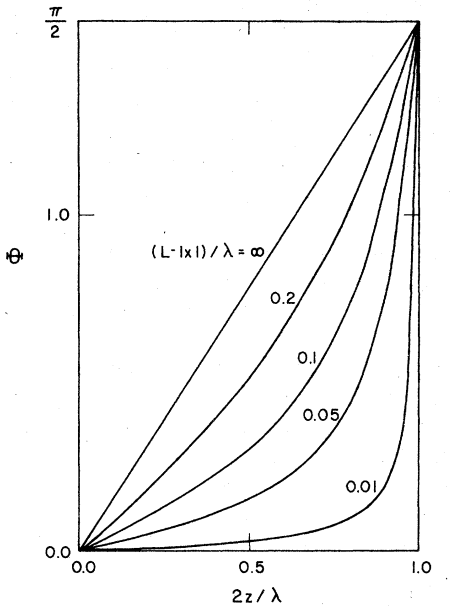

FIG. 2. Director angle $\Phi(x,z;\infty)$ in radians, as given by Eq. (2.3), as a function of z in the range of $0<z<\frac{1}{2}\lambda$, for $(L-x)/\lambda=0.01,\ 0.05,\ 0.1,\ 0.2,\ \infty$.

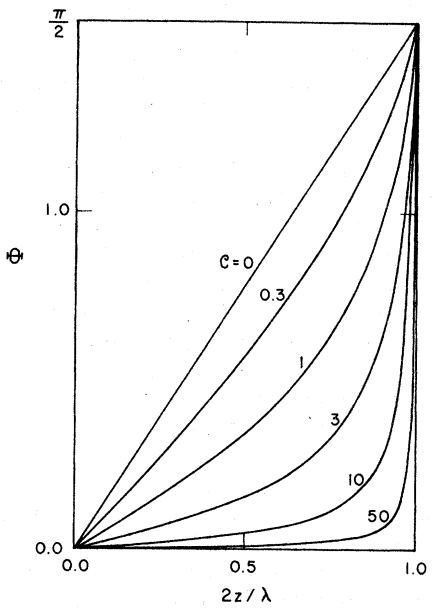

FIG. 3. Director angle $\Phi(L,z;\mathcal{C})$ in radians as given by Eq. (2.5) as a function of z in the range $0<z<\frac{1}{2}\lambda$, for $\mathcal{C}=0,0.3,1,3,10,50$.

values of $\mathcal{C}$. In Appendix B we show that if $L\geq 2\lambda$, Eq. (2.1) may be rewritten as

$$\Phi(x,z;\mathcal{C})=\tan^{-1}[\tan(qz)\tanh q(L-|x|)]$$
$$+e^{-2q(L-|x|)}\sin(2qz)$$
$$\times\int_0^1 dt\,\frac{t^{\mathcal{C}}}{1+2te^{-2q(L-|x|)}\cos 2qz+t^2e^{-4q(L-|x|)}}\,. \tag{2.4}$$

We examine first the behavior of Φ along the plate face $x=L$. In this case Eq. (2.4) reduces to

$$\Phi(L,z;\mathcal{C})=\sin(2qz)\int_0^1 dt\,\frac{t^{\mathcal{C}}}{1+2t\cos 2qz+t^2} \tag{2.5}$$
$$(0<z<\tfrac{1}{2}\lambda)$$

We have used standard numerical methods to evaluate the integral in Eq. (2.5) as a function of z for assorted values of $\mathcal{C}$, and our results for Φ are shown in Fig. 3. It will be noted that $\mathcal{C}=3$ might be taken as the dividing line between small and large values of $\mathcal{C}$. For $\mathcal{C}>3$, the quantity $\Phi(L,z)$ initially rises slowly with z and then, for z approaching $\frac{1}{2}\lambda$, rises steeply to the value $\frac{1}{2}\pi$. In the limiting case $\mathcal{C}\to\infty$, $\Phi(L,z)$ is discontinuous at $z=\frac{1}{2}\lambda$, in agreement with what we have seen already in Fig. 2. By contrast, for $\mathcal{C}<3$ the weak interaction of the plate with the molecules modifies Φ only slightly from its form $\Phi=\pi z/\lambda$ for bulk cholesteric.

For the general case $|x|<L$, the results for $\Phi(x,z;\mathcal{C})$, obtained by numerical integration of Eq. (2.4), are shown in Figs. 4, 5, and 6 for $\mathcal{C}=3,10$, and 50, respectively. The most interesting feature of these families of curves, as well as that of Fig. 2 which applies for $\mathcal{C}=\infty$, is that at distances from the plate faces exceeding about 0.3λ the director angle already closely approximates its bulk value. That is, the effects of the surface

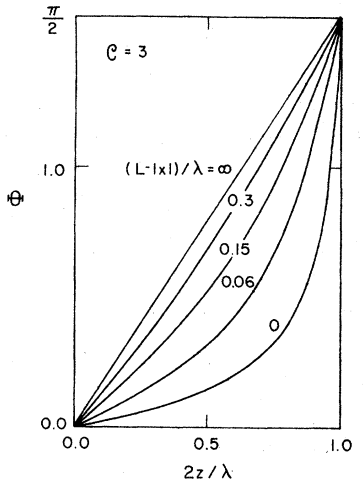

FIG. 4. Director angle $\Phi(x,z;\mathcal{C})$ in radians, as given by Eq. (2.4), for $\mathcal{C}=3$ and $(L-|x|)/\lambda=0,0.06,0.15,0.3,\infty$.

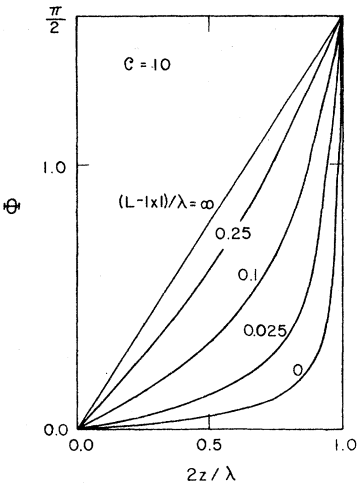

FIG. 5. Same as in Fig. 4, but for $\mathfrak{C}=10$, and $(L-|x|)/\lambda=0$, 0.025, 0.1, 0.25, ∞.

interaction extend over a characteristic distance of order 0.3λ from the plate faces, and this characteristic distance is essentially independent of the value of $\mathfrak{C}$. It is interesting that the analytic expressions for Φ of Eqs. (2.1) and (2.4) are both particularly opaque as regards the existence of this characteristic length.

We now derive a useful approximate expression for Φ which applies when $\mathfrak{C}\gg 1$ and $|x|<L$. For such values of $\mathfrak{C}$ the integrand in Eq. (2.4) is extremely small except in the immediate vicinity of $t=1$. As such it is a good approximation to replace the denominator by its value at the upper limit. (The exception is for $x=\pm L$, since if $z=\frac{1}{2}\lambda$, the denominator vanishes at the upper limit.) The resulting integral is then readily evaluated and we obtain

$$\Phi(x,z;\mathfrak{C})\simeq\Phi(x,z;\infty)+\frac{1}{\mathfrak{C}}\left(\frac{e^{-2q(L-x)}\sin 2qz}{1+2e^{-2q(L-x)}\cos(2qz)+e^{-4q(L-x)}}+(x\to -x)\right)\quad(|x|<L). \tag{2.6}$$

At this point we remark that for $\mathfrak{C}=\infty$ the director field can be described in terms of a periodic array of line disclinations which are situated on the plate faces at $z_n=(n+\frac{1}{2})\lambda, n=0,\pm1,\ldots$. The appropriateness of this description is most simply confirmed by noting that for $z\simeq\frac{1}{2}\lambda$ and $L-|x|\ll\lambda$, the director angle, as given by Eq. (2.3), reduces to

$$\Phi(x,z;\infty)\simeq\tan^{-1}[(L-|x|)/(\tfrac{1}{2}\lambda-z)], \tag{2.7}$$

which is the familiar form of a line disclination[18] situated at $x=\pm L$ and $z=\frac{1}{2}\lambda$. For finite but large values of $\mathfrak{C}$ the extremely rapid variation of Φ with z along the plate faces is suggestive of a periodic array of surface disclinations whose cores are smeared symmetrically over a short distance Δz ($\ll\frac{1}{2}\lambda$) about the lines $z_n=(n+\frac{1}{2})\lambda$. The analogous behavior in nematics, with finite surface interaction, has been studied in detail by Meyer[19] and Vitek and Kléman.[20]

Thus far we have assumed that the plate spacing is larger than the pitch; in particular, Eqs. (2.2)–(2.6) are applicable only if this condition is met. Starting from Eq. (2.1), and employing the Poisson summation formula, one can derive the following exact expression[21] for Φ,

$$\Phi(x,z)=\pi\mu\sum_{n=1}^{\infty}\frac{1}{y_n^2+\mu^2+\mu}\frac{\cos(y_n x/L)}{\cos y_n}\frac{\sinh(y_n z/L)}{\sinh(y_n\lambda/2L)}\quad(-\tfrac{1}{2}\lambda<z<\tfrac{1}{2}\lambda). \tag{2.8}$$

Here the quantities $y_n, n=1,2,\ldots$, are the positive real roots of

$$y_n\tan y_n=\mu \tag{2.9}$$

and $\mu=CL/K$. For the regime $\lambda>L$, highly accurate[22] values of Φ can be obtained by ignoring all but the first few terms of the series in Eq. (2.8).

The results of this section can be summarized as follows. For large plate spacings ($L>\lambda$), within a distance of approximately 0.3λ of the plate faces, the surface interaction causes the director angle to increase very slowly with z, from $\Phi=0$ at $z=0$, until the vicinity of $z=\frac{1}{2}\lambda$, where Φ increases sharply, passes through the value $\frac{1}{2}\pi$ for $z=\frac{1}{2}\lambda$,

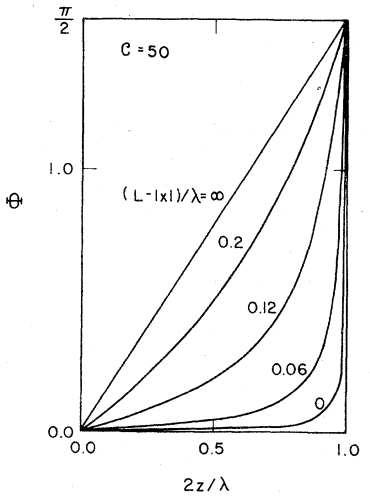

FIG. 6. Same as in Fig. 4, but for $\mathfrak{C}=50$ and $(L-|x|)/\lambda=0$, 0.012, 0.06, 0.2.

and reaches π shortly thereafter. Beyond 0.3λ from the plate faces, Φ increases essentially linearly with z, as in bulk cholesteric with pitch 2λ. For the case $\lambda > L$, even in the center of the cholesteric, the dependence of Φ on z resembles, although in less extreme form, that along the plate faces.

The above-mentioned properties of the director angle could be investigated employing optical interference techniques.[23] So far only the gross features have been explored experimentally for several fixed plate spacings as the storage mode undergoes a transition to the nematic state induced by an external field.[11]

III. EXACT EULER EQUATIONS

In Sec. II it was assumed that the director lies in the xy plane, perpendicular to the plates-cholesteric sandwich. We show below, in Sec. III C, by numerical solution of the exact Euler equations, that in the strong anchoring case this assumption is essentially valid except in the immediate vicinity of the plates. The maximum departure of $\vec{n}$ from the xy plane is approximately 7°.

A. Director field equations

The Frank free-energy density of a left-handed cholesteric liquid crystal in the one-constant approximation ($K_1 = K_2 = K_3 = K$) is[24]

$$F = \tfrac{1}{2} K[(\nabla \cdot \vec{n})^2 + (\vec{n} \cdot \nabla \times \vec{n})^2 + (\vec{n} \times \nabla \times \vec{n})^2 - 2q_0 \vec{n} \cdot \nabla \times \vec{n}], \tag{3.1}$$

where $q_0 = \pi/\lambda_0$ and $2\lambda_0$ is the pitch of the bulk cholesteric. The equilibrium director field is obtained by minimizing the total free energy with respect to all variations of $\vec{n}$, while maintaining the constraint $|\vec{n}(\vec{r})| = 1$ for all $\vec{r}$. The resulting Euler equation is given by

$$\nabla^2 \vec{n} + 2q_0 \nabla \times \vec{n} = L(\vec{r}) \vec{n}(\vec{r}), \tag{3.2}$$

where $L(\vec{r})$ is a Lagrange multiplier function originating from the local constraint $|\vec{n}| = 1$. It proves simpler to eliminate the unknown function $L(\vec{r})$ by writing the following equation, which is equivalent to (3.2),

$$\vec{n} \times (\nabla^2 \vec{n} + 2q_0 \nabla \times \vec{n}) = 0. \tag{3.3}$$

In order to satisfy the constraint $|\vec{n}| = 1$, we express the components of $\vec{n}$ in terms of the two angles $\Phi(x,z)$ and $\alpha(x,z)$ (see Fig. 1), according to the relations

$$\begin{aligned} n_x &= \sin\Phi(x,z)\cos\alpha(x,z), \\ n_y &= \cos\Phi(x,z)\cos\alpha(x,z), \\ n_z &= \sin\alpha(x,z). \end{aligned} \tag{3.4}$$

It is then straightforward to show that Eq. (3.3) is equivalent to the following pair of coupled nonlinear partial differential equations:

$$\nabla^2\alpha = 2q_0 \cos^2\alpha \sin\Phi \frac{\partial\Phi}{\partial x} - \left((\nabla\Phi)^2 - 2q_0 \frac{\partial\Phi}{\partial z}\right) \sin\alpha \cos\alpha, \tag{3.5a}$$

$$-(\cos\alpha)\nabla^2\Phi + 2\sin\alpha(\nabla\alpha \cdot \nabla\Phi) = 2q_0 \left(\sin\alpha \frac{\partial\alpha}{\partial z} + \cos\alpha \sin\Phi \frac{\partial\alpha}{\partial x}\right). \tag{3.5b}$$

As discussed in Sec. II, in Ref. 12 the Frank free energy was minimized while constraining the angle α to be identically zero. The resulting Euler equation was found to be $\nabla^2\Phi = 0$. However, as is seen from Eqs. (3.5a) and (3.5b), the assumption $\alpha \equiv 0$ is tenable only if both $\nabla^2\Phi = 0$ and $\partial\Phi/\partial x = 0$.[10] In fact, for the solution Eq. (2.1) of $\nabla^2\Phi = 0$, the quantity $\partial\Phi/\partial x$ is not identically zero. Thus the equation $\nabla^2\Phi = 0$ defines a set of functions which minimize the Frank free energy when one restricts variations of $\vec{n}$ to within the subspace with $\alpha = 0$. However, these solutions do *not* minimize the free energy for the full space of variations of $\vec{n}$ which encompasses arbitrary Φ and α.

As stated in Sec. I, we have chosen the interaction between the plate faces and the cholesteric so that the following boundary conditions apply:

$$\alpha(x = \pm L, z) = 0 \tag{3.6}$$

and

$$\frac{\partial\Phi}{\partial x}(\pm L, z) = \mp \frac{C}{K} \Phi(\pm L, z). \tag{3.7}$$

In addition, for a left-handed cholesteric with pitch 2λ, the director must satisfy the requirements

$$\Phi(x, z + \lambda) = \pi + \Phi(x, z), \tag{3.8}$$

$$\alpha(x, z + \lambda) = -\alpha(x, z). \tag{3.9}$$

The solutions of the differential equations (3.5a) and (3.5b), supplemented with the boundary conditions Eqs. (3.6)–(3.9), possess the following symmetry properties[15]

$$\Phi(-x, z) = \Phi(x, z) = -\Phi(x, -z), \tag{3.10}$$

$$-\alpha(-x, z) = \alpha(x, z) = \alpha(x, -z). \tag{3.11}$$

In view of Eqs. (3.8)–(3.11), it is sufficient to solve Eqs. (3.5a) and (3.5b) for the restricted region $0 < x < L$, $0 < z < \frac{1}{2}\lambda$. For this restricted region, the full set of boundary conditions to be satisfied are given by

$$\frac{\partial \alpha}{\partial z} = 0, \Phi = 0 \quad (0 < x < L, z = 0), \tag{3.12}$$

$$\alpha = 0, \frac{\partial \Phi}{\partial x} = -\left(\frac{C}{K}\right)\Phi \quad (x = L, 0 < z < \tfrac{1}{2}\lambda), \tag{3.13}$$

$$\alpha = 0, \Phi = \tfrac{1}{2}\pi \quad (0 < x < L, z = \tfrac{1}{2}\lambda), \tag{3.14}$$

$$\alpha = 0, \frac{\partial \Phi}{\partial x} = 0 \quad (x = 0, 0 < z < \tfrac{1}{2}\lambda). \tag{3.15}$$

B. Approximate analytical solution

In this and the following subsection we shall restrict our attention to the limiting case of $\mathcal{C} = \infty$, corresponding to the strong anchoring of the molecules, along the y axis (see Fig. 1), at the plate faces. As remarked above, the choice $\alpha \equiv 0$ is not a solution of Eq. (3.5a) if $\partial\Phi/\partial x$ is nonzero. Further, we expect that $\partial\Phi/\partial x$ will increase monotonically with increasing values of $\mathcal{C}$. Thus the choice $\mathcal{C} = \infty$ should correspond to an upper bound for the angle $\alpha(x,z)$. For this case, Eq. (3.13) can be replaced by the simpler form

$$\alpha = \Phi = 0 \quad (x = L, 0 < z < \tfrac{1}{2}\lambda) \tag{3.16}$$

whereas the other boundary conditions, given by Eqs. (3.12), (3.14), and (3.15) remain unchanged.

Some of the essential qualitative features of the function α can be established by an approximate analytic treatment which we now describe. Of course, to obtain quantitatively accurate solutions of the complex nonlinear equations of Eq. (3.5) we have no alternative but to employ numerical methods, as discussed in subsection C. The approximation procedure we adopt here consists of (i) solving Eq. (3.5b) for Φ when α is set equal to zero, (ii) substituting the result for Φ in the right-hand side of Eq. (3.5a), and then solving the resulting equation for α after linearizing terms dependent on α.

1. Region $L - 0.1\lambda \lesssim |x| \leqslant L$, $0 < \frac{\lambda}{2} - z \lesssim 0.1\lambda$

We shall first confine our attention to the restricted region $L - 0.1\lambda \lesssim |x| \leq L$ and $0 < \frac{1}{2}\lambda - z < 0.1\lambda$. It is in this region that the driving term $\partial\Phi/\partial x$ of Eq. (3.5a), and therefore $\nabla^2\alpha$ as well, assumes its largest value. Because of the fact that $\alpha(x,z)$ is an odd function of x [see Eq. (3.11)] it is sufficient to consider positive values of x. The relevant solution for Φ in this region is given by Eq. (2.3), or its simplified form

$$\Phi \simeq \tan^{-1}[(L - x)(\tfrac{1}{2}\lambda - z)^{-1}]. \tag{3.17}$$

It is convenient to introduce polar coordinates defined by the equation

$$L - x = r\sin\theta, \quad \tfrac{1}{2}\lambda - z = r\cos\theta, \tag{3.18}$$

and we stress that we are interested in values of r small compared to λ, and angles θ in the interval $(0, \frac{1}{2}\pi)$. Equation (3.5a) then reduces to the following simplified form:

$$\nabla^2\alpha = -\frac{q_0}{2r}(1 + \cos 2\alpha)\sin 2\theta - \frac{1}{2r^2}\sin 2\alpha. \tag{3.19}$$

Furthermore, the boundary conditions for α are

$$\alpha(r, 0) = \alpha(r, \tfrac{1}{2}\pi) = 0. \tag{3.20}$$

Now it will be noted that Eq. (3.19) is invariant under the change of variables $r \to -r$, $\alpha \to -\alpha$. Thus we can write

$$\alpha(r, \theta) = \sum_{n=0}^{\infty} (q_0 r)^{2n+1} f_{2n+1}(\theta), \tag{3.21}$$

where, because of Eq. (3.20), the functions f_{2n+1} satisfy the requirements

$$f_{2n+1}(0) = f_{2n+1}(\tfrac{1}{2}\pi) = 0. \tag{3.22}$$

Substitution of Eq. (3.21) for α in Eq. (3.19) leads to an infinite set of ordinary differential equations for the angular functions. We shall not bother to write down these equations since for small r, which is the region we are considering, it is sufficient to retain only the first term $q_0 r f_1(\theta)$; the second term is of order $(q_0 r)^3$ and thus may safely be ignored. It is then straightforward to show that f_1 satisfies the equation

$$f_1'' + 2f_1 = -\sin 2\theta, \tag{3.23}$$

and its solution satisfying Eq. (3.22) is

$$f_1(\theta) = \tfrac{1}{2}\sin 2\theta. \tag{3.24}$$

Thus we arrive at the following approximate result for α, written in terms of the original spatial coordinates,

$$\alpha(x, z) = q_0(L - x)(\tfrac{1}{2}\lambda - z)[(L - x)^2 + (\tfrac{1}{2}\lambda - z)^2]^{-1/2}. \tag{3.25}$$

The most important feature of this result is that the family of α curves versus z, corresponding to differing values of x, have a common tangent, the straight line $q_0(\frac{1}{2}\lambda - z)$, as $z \to \frac{1}{2}\lambda$. As shown in subsection C, this property of α is in fact exhibited by the numerical solution for α. We emphasize that Eq. (3.25) can be used only for small values of both $(L - x)/\lambda$ and $(\frac{1}{2}\lambda - z)/L$, for otherwise the simplified form Eq. (3.17) for Φ is invalid.

2. Region $0 \leqslant |x| \lesssim L - \lambda$, $0 \leqslant z \leqslant \frac{1}{2}\lambda$

An approximate solution of Eq. (3.5a) can also be derived without difficulty for the region $0 \leq |x| \lesssim L - \lambda$. Once again we remind the reader of the fact that $\alpha(x,z)$ is an odd function of x and

thus it suffices to consider the region $0 \leq x \lesssim L - \lambda$. For this region we have $\tanh q(L-x) \simeq 1 - 2e^{-2q(L-x)}$, and thus Eq. (2.3) may be rewritten as

$$\Phi \simeq \tan^{-1}[(1 - e^{-2q(L-x)}) \tan qz] . \tag{3.26}$$

Thus the derivatives $\partial\Phi/\partial x$ and $(\nabla\Phi)^2 - 2q_0 \partial\Phi/\partial z$ which appear in Eq. (3.5a) are well approximated as $\partial\Phi/\partial x = -4q \sin qz \cos qz e^{-2q(L-x)}$ and $(\nabla\Phi)^2 - 2q_0 \partial\Phi/\partial z \simeq q^2 - 2qq_0$. Now in view of the smallness of the term $\partial\Phi/\partial x$, because of the factor $e^{-2q(L-x)}$, we can expect that α will be very small in this region of the cholesteric, and thus $\cos^2\alpha \simeq 1$ and $\sin\alpha \cos\alpha \simeq \alpha$. We thus arrive at the following approximate, linear equation for α

$$\nabla^2\alpha - q(2q_0 - q)\alpha = -8qq_0 \sin^2 qz \cos qz e^{-2q(L-x)} . \tag{3.27}$$

Although this equation is an accurate approximation to Eq. (3.5a) only for the region $L - x \gtrsim \lambda$, we shall, nevertheless, arbitrarily employ it for the wider region $0 \leq x \leq L$, so as to utilize the boundary conditions Eqs. (3.12) and (3.14)–(3.16). Confining our attention to the special case $q = q_0$, it is then straightforward to verify that Eq. (3.27) and the stated boundary conditions are satisfied by

$$\begin{aligned}\alpha(x,z) = {} & \{\exp[-q_0\sqrt{2}(L-x)] \\ & - \exp[-2q_0(L-x)]\} \cos q_0 z \\ & + \tfrac{1}{3}\{\exp[-q_0\sqrt{10}(L-x)] \\ & - \exp[-2q_0(L-x)]\} \cos 3q_0 z .\end{aligned} \tag{3.28}$$

The most important feature of this result is the exponential decrease of $\alpha(x,z)$ as one proceeds from the plate at $x = L$ towards the interior of the cholesteric. In Fig. 7 are shown curves of $\alpha(x,z)$, as given by Eq. (3.28), as a function of z for several values of x within a distance λ_0 of the plate at $x = L$. It is interesting to note that the curves shown embody the same qualitative features as those exhibited by the exact numerical solution of Eq. (3.5) (see Fig. 8) even though, as explained above, Eq. (3.27) is expected to be a good approximation to Eq. (3.5a) only for $x < L - \lambda_0$.

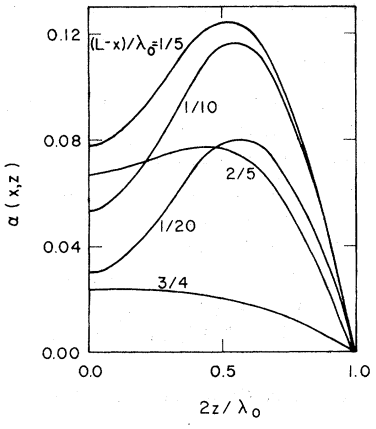

FIG. 7. Angle $\alpha(x,z)$ in radians, as given by the approximate analytical formula of Eq. (3.28) for the strong anchoring limit. The curves shown are for $(L-x)/\lambda_0 = \frac{1}{20}, \frac{1}{10}, \frac{1}{5}, \frac{2}{5}, \frac{3}{4}$.

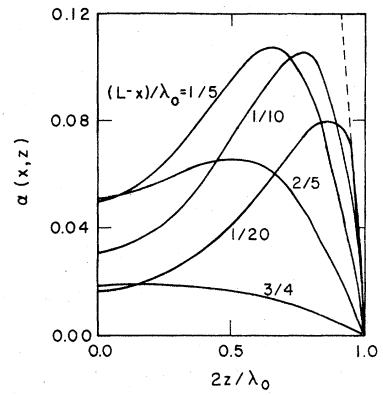

FIG. 8. Angle $\alpha(x,z)$ in radians, as obtained by numerical solution of Eqs. (3.5a), and (3.5b) for the strong anchoring limit. The curves shown are for $(L-x)/\lambda_0 = \frac{1}{20}, \frac{1}{10}, \frac{1}{5}, \frac{2}{5}, \frac{3}{4}$. If $(L-x)/\lambda_0 \lesssim 0.2$, the family of curves is predicted [see Eq. (3.25)] to have the common tangent $\alpha = \frac{1}{2}\pi - \pi z/\lambda_0$, as $z \to \frac{1}{2}\lambda_0$, shown as the dashed line.

C. Numerical results

We here describe the numerical solution of Eq. (3.5) in the case where the boundary conditions are given by Eqs. (3.12) and (3.14)–(3.16), that is, where the molecules at the plate faces are anchored in the y direction. In the following we have taken the pitch of the cholesteric to be $2\lambda_0$. The first step consists of replacing the region $0 < x < L$, $0 < z < \frac{1}{2}\lambda_0$ by a uniform 30×30 grid of points within the smaller region $L - \frac{3}{2}\lambda_0 < x < L$, $0 < z < \frac{1}{2}\lambda_0$. In light of the results of Secs. II and III B 2 we believe that it is justified to regard the plane $x = L - \frac{3}{2}\lambda_0$ as sufficiently deep within the cholesteric so that we can require that $\alpha = 0$ and $\Phi = (\pi/\lambda_0)z$ on this plane. The pair of differential equations of Eq. (3.5) are then replaced by their usual finite-difference expressions. To solve these equations we have utilized the method of alternating directions[25] in conjunction with the following iterative scheme. The $(n+1)$th-order estimate $\alpha_{n+1}(x,z)$ is obtained by solving Eq. (3.5a) with Φ and α on the right-hand side replaced by Φ_n and α_n, respectively.

Similarly, the $(n+1)$th-order estimate $\Phi_{n+1}(x,z)$ is obtained by solving Eq. (3.5b) where α_{n+1} and Φ_{n+1} are substituted for α and Φ, with the exception of the nonlinear factor $\sin\Phi$ on the right-hand side which is replaced by $\sin\Phi_n$. The lowest-order estimates are chosen as follows: $\alpha_0 \equiv 0$, and Φ_0 is the solution of $\nabla^2\Phi_0 = 0$ satisfying the boundary conditions (3.12) and (3.14)–(3.16). The iterative procedure is repeated successively until convergence is achieved. All calculations were performed using the Bar-Ilan University IBM 370-168 computer. In practice, less than ten iterations proved to be sufficient to insure convergence.

Our numerical results for α are shown in Fig. 8. Note that the largest values of α ($\simeq 0.11$ rad, i.e. $\simeq 7°$) occur in the immediate vicinity of the plate faces, and α rapidly decreases to zero as one proceeds towards the center of the cholesteric sandwich. Note further that in the vicinity of $z = \frac{1}{2}\lambda_0$ the family of curves tend to zero, and for $(L-x)/\lambda \lesssim \frac{1}{5}$ possess the common tangent $q_0(\frac{1}{2}\lambda_0 - z)$, shown as a solid straight line in Fig. 8. This property is in accord with our theoretical result, given above by Eq. (3.25), derived by linearizing Eq. (3.5a) in the vicinity of $z = \frac{1}{2}\lambda_0$ and $x = L$. The smallness of α everywhere except in the immediate vicinity of $z = \frac{1}{2}\lambda_0$ and $x = L$ can be attributed to three specific causes. First, the choice of boundary conditions requires α to vanish along three edges ($x = L, x = L - \frac{3}{2}\lambda_0, z = \frac{1}{2}\lambda_0$) of the four comprising the boundary. Second, outside this restricted region, the driving term $\partial\Phi/\partial x$ in Eq. (3.5a) is very small. Third, even where $\partial\Phi/\partial x$ is large, the nonlinear terms in Eq. (3.5a) tend to suppress all attempts by α to grow.

Concerning the angle $\Phi(x,z)$, we have found that its value is only very slightly different from $\Phi_0(x,z)$, the value of Φ when α is constrained to be identically zero throughout the cholesteric sandwich. As such we refer the reader back to Fig. 2.

Cladis and Kléman[10] have argued that the usage of the constrained solution $\vec{n}_0(\vec{r})$, with the angle α identically zero, is unwarranted. Their argument may be summarized as follows. Defining the differential operator $H = \nabla^2 + 2q_0\nabla\times$, Eq. (3.2) may be written as

$$\vec{n}(\vec{r}) = H\vec{n}(\vec{r}) / |H\vec{n}(\vec{r})|, \tag{3.29}$$

having used the fact that $|\vec{n}(\vec{r})| = 1$. They then argue that $\vec{n}_0$ will be a good approximation to the exact solution $\vec{n}$ of Eq. (3.29) if $H\vec{n}_0(\vec{r})/|H\vec{n}_0(\vec{r})| \equiv \vec{n}_1(\vec{r})$ is nearly equal to $\vec{n}_0$. In fact, they have found that there exist regions in the cholesteric where $n_{1z}^2(\vec{r}) > n_{1x}^2(\vec{r}) + n_{1y}^2(\vec{r})$, in contrast to the approximant $\vec{n}_0(\vec{r})$, for which $n_{0z} \equiv 0$. As we discuss below, this behavior of $\vec{n}_1$ does *not* detract from the usefulness of the planar solution $\vec{n}_0$. The form of Eq. (3.29) suggests that we define a sequence of approximants $\vec{n}_l(\vec{r})$ according to the relation

$$\vec{n}_{l+1}(\vec{r}) = H\vec{n}_l(\vec{r}) / |H\vec{n}_l(\vec{r})| \quad (l = 0, 1, 2, \ldots), \tag{3.30}$$

where $\vec{n}_0(\vec{r}) = \hat{x}\sin\Phi_0(x,z) + \hat{y}\cos\Phi_0(x,z)$ and Φ_0 is given by Eq. (2.3). We have found that the sequence of approximants fails to converge to any unique function of $\vec{r}$ for increasing values of l, and thus fails to converge to the exact numerical solution of Eq. (3.2). As we have seen above, the exact solution of Eq. (3.2) in the strong anchoring case is indeed very similar to $\vec{n}_0(\vec{r})$ and in particular the z component of $\vec{n}$ is very small compared to unity.

The main result of this section is that the director is very nearly confined to the xy plane, i.e., the plane perpendicular to the plates at $x = \pm L$. The departure of the director from this plane is largest in the immediate vicinity, within a distance of order λ_0, of the plates, and its maximum value is about 7°. We therefore suggest that a sufficiently accurate theoretical description of the cholesteric storage mode is provided by the model discussed in Ref. 12 and Sec. II of the present article, based on the simplified description of the director being confined to the xy plane. The discussions of the electric capacitance and lifetime of the storage mode, given in the following sections, is based on this simplified description.

IV. ELECTRICAL CAPACITANCE

A macroscopic probe of the director field is provided by electrical capacitance measurements.[8,9] Let C_G, C_{SM}, and C_H denote the electrical capacitance of the system when a weak electric field is applied perpendicular to the cholesteric-plates sandwich (i.e., in the x direction) for the three specific configurations: stable cholesteric (Grandjean mode), storage mode, and homeotropic ordering. The latter two configurations are created successively from the stable cholesteric mode by applying an external magnetic field of sufficient strength in the x direction, i.e., also perpendicular to the sandwich (see Refs. 8 and 9 for details). Following Hulin's notation, we define a quantity R by the relation

$$R = (C_G - C_{SM})/(C_G - C_H). \tag{4.1}$$

This quantity is related to the equilibrium director angle $\bar{\Phi}(x,z)$ of the storage mode by the approximate equality[26]

$$R(\lambda_0/L;e) \simeq \frac{1}{2L\lambda}\int_{-L}^{L} dx \int_{-\lambda/2}^{\lambda/2} dz \sin^2\bar{\Phi}(x,z). \tag{4.2}$$

For the case $L/\lambda_0 \gg 1$, except in the immediate

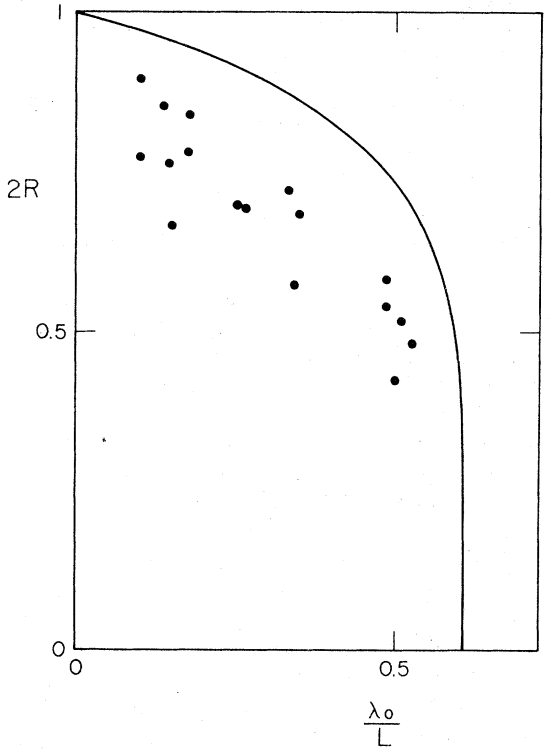

FIG. 9. Theoretical capacitance ratio $2R$, defined by Eqs. (4.1) and (4.2), versus λ_0/L. Experimental points are due to Hulin (Ref. 9).

vicinity of the plate faces, $\bar{\Phi}$ is given by $\bar{\Phi}=(\pi/\lambda_0)z$ and thus $R=\frac{1}{2}$. On the other hand, as L is decreased towards the critical spacing, $\bar{\Phi}\simeq 0$ and then $R\to 0$.

In Fig. 9 we have reproduced Hulin's experimental results[9] for $2R$ as a function of λ_0/L for mesomorphic mixtures of small concentrations of cholesteryl nonanoate (CN) in MBBA. The dependence of $2R$ on λ_0/L according to the present theory is shown by the solid curve. This was obtained by employing standard numerical integration methods in conjunction with Eqs. (2.1) or (2.8). The values of $\bar{\lambda}$, appropriate to given plate spacing were taken from Ref. 12. The following choices were made for the relevant parameters: $2\lambda_0=16.5$ μm (see Ref. 27); $C=0.10$ erg/cm^2 (see Sec. V); $K_2=2.2\times10^{-7}$ dyn (Ref. 8); $K_1=K_3=6.0\times10^{-7}$ dyn (this is roughly the average of the values $K_1=5.3\times10^{-7}$ dyn and $K_3=7.5\times10^{-7}$ dyn, estimated in Ref. 8). Variations of C, ranging from 0.05 to 0.2 erg/cm^2, or of K_2 and K_3, within the experimental uncertainty ($\simeq$10%) quoted in Ref. 8, affect the theoretical estimate of $2R$ only by several percent.

A simple approximate analytic expression for R, which is highly accurate for the regime $L\geq 2\bar{\lambda}(L,\mathcal{C})$, when $\mathcal{C}\gg 1$, is obtained by substituting Eq. (2.3) for the director angle in Eq. (4.2). We then have that

$$\sin^2\bar{\Phi}=\frac{1}{2}\left(1-\frac{1+\cos(2\bar{q}z)\cosh 2\bar{q}(L-|x|)}{\cos(2\bar{q}z)+\cosh 2\bar{q}(L-|x|)}\right), \tag{4.3}$$

$$\int_{-\bar{\lambda}/2}^{\bar{\lambda}/2} dz\,\sin^2\Phi=\tfrac{1}{2}\lambda(1-e^{2\bar{q}(L-|x|)}), \tag{4.4}$$

and finally,

$$2R\simeq 1-\bar{\lambda}(L)/2\pi L \quad (L\geq 2\bar{\lambda}). \tag{4.5}$$

For the choice of parameters given above $\mathcal{C}\simeq 33$ and thus Eq. (4.5) should be relevant for the range $L\geq 2\bar{\lambda}$. This result for $2R$ has been derived for the choice $K_1=K_2=K_3$. Using the transcription given in detail in Appendix A for a system where $K_1=K_3\neq K_2$, Eq. (4.5) is replaced by

$$2R\simeq 1-(K_1/K_2)^{1/2}\bar{\lambda}(L)/2\pi L \quad (L\geq 2\bar{\lambda}). \tag{4.5'}$$

By contrast, Hulin[9] has suggested that his data, which extends over the range $L/\lambda_0\geq 2$, satisfy the empirical formula $2R=1-\lambda_0/L$. The agreement seems reasonable in view of the fact that the discrepancy between our theoretical curve and Hulin's empirical formula is of order of the scatter of the experimental points.

V. LIFETIME OF THE STORAGE MODE

The lifetime τ of the storage mode as a function of L/λ_0 has been measured by Hulin[9] for mesomorphic mixtures of CN in MBBA. Lifetimes ranging from several days down to of order 1 min were obtained by reducing the value of L/λ_0 from 14 to 2. We have reproduced Hulin's data points in Fig. 10. For times exceeding τ, the cholesteric sandwich was found to be in the stable Grandjean configuration, i.e., helix axis perpendicular to the plates. Although there is considerable scatter in the experimental data, Hulin noted that a reasonable fit exists with the empirical formula $\tau=0.5e^{-0.69L/\lambda_0}$, where τ is measured in minutes. However, Hulin did not propose a model which accounts for this behavior.

A satisfactory theory of the dependence of τ on L/λ_0 must take into account the passage of the system from the metastable storage mode to the stable cholesteric configuration, where the helix axis points perpendicular to the confining plates. We propose the following sequence of events for this process. Suppose that as a result of thermal fluctuations a small element of volume V initially in the storage mode configuration were to unwind to the nematic configuration. This would entail an increase in the free energy of the system by an

amount $V|F|$, where $F(<0)$ is the free energy per unit volume in the storage mode as measured with respect to the nematic configuration. If the volume of this region is less than some critical volume V_c it is plausible that the neighboring environment will act to restore the original metastable state. However, if V exceeds V_c we expect that the small nematic region will rewind into the stable cholesteric configuration, entailing a decrease of the free energy, and trigger the same chain of events in the immediate environment. In this fashion the storage mode will swiftly pass over to the stable cholesteric configuration, via the nematic configuration, with the concomitant lowering in free energy. These considerations suggest the following phenomenological formula for the lifetime of the storage mode:

$$\tau(L)=\tau_0\{\exp[V_c|F(L)|/k_BT]-1\}, \qquad (5.1)$$

where τ_0 is a characteristic dissipative time. The quantity $\exp[V_c|F(L)/k_BT]$ is inversely proportional to the probability that a region of volume V_c will acquire the requisite free energy to pass to the nematic phase. The dependence of τ on the plate spacing $2L$ enters via $F(L)$. Finally, we have subtracted unity from the exponential so that the lifetime of the storage mode will equal zero if the difference in free energy F between the storage mode and the nematic phases is zero.

We have used the results of Ref. 12 for $F(L)$, adapted to the case $K_1=K_3\neq K_2$, and the numerical values of K_2 and K_3 given at the end of Sec. IV of the present article. The surface energy constant C and the parameters τ_0 and V_c in Eq. (5.1) were varied so as to obtain the best least-squares fit to Hulin's experimental data. The results of our analysis are $C=(0.1\pm0.05)\text{erg/cm}^2$, $\tau_0\simeq 40$ sec, and $V_c\simeq(1\ \mu\text{m})^3$. Essentially the same quality fit is obtained if τ_0 is varied by about a factor of 2 and V_c is simultaneously readjusted by about 30%. In Fig. 10, we have reproduced Hulin's data points for τ as a function of L/λ_0 and have superimposed our theoretical curve. The agreement is fairly good and argues for the plausibility of our proposed mechanism for the lifetime of the storage mode. Finally, note that Hulin's data suggest that the critical value of L/λ_0 is about 1.7. That is, for plate spacings $2L\approx 3.4\lambda_0$ the storage mode is unstable. This is in good agreement with the theoretical critical ratio (see Ref. 12) which lies in the range $1.6<L_c/\lambda_0<2.0$ for the relevant span of acceptable values of C and the chosen values of K_2 and K_3.

VI. SUMMARY

The major topic considered in this article is the detailed spatial dependence of the director field $\vec{n}(\vec{r})$ of the metastable cholesteric storage mode. An analytic and numerical study of the exact Euler equations shows that the director is very nearly confined to the xy plane, i.e., perpendicular to the plate-cholesteric sandwich. The maximum departure of $\vec{n}$ from this plane is less than 7° and this occurs within the immediate vicinity of the plates. As one proceeds towards the interior of the cholesteric, the component n_z decreases to zero exponentially, with a characteristic length of order the pitch $2\lambda_0$. This result enables one to adopt the simplifying description, of a planar director $\vec{n}(\vec{r})=\hat{x}\sin\Phi(x,z)+\hat{y}\cos\Phi(x,z)$, of the theoretical model of Ref. 12. We have presented detained analytic and numerical results for the director angle Φ for a large variety of cases. In particular, as long as the plate spacing is larger than the equilibrium pitch of the cholesteric for that spacing, one can employ Eq. (2.4). If, further, the dimensionless surface energy coefficient $\mathcal{C}=C\lambda_0/(2\pi K)$ is large compared to unity, one can employ the simpler expression Eq. (2.6). In the strong anchoring limit ($C\to\infty$), Φ is given by the simple expression of Eq. (2.3). For the regime where the pitch of the storage mode exceeds that of the plate spacing, the first few terms of Eq. (2.8) provide a highly accurate approximation to the director angle.

We have also calculated the dependence of the electrical capacitance of the cholesteric on plate spacing. Specifically, the calculation involves the spatial average of n_x^2. Thus a comparison between

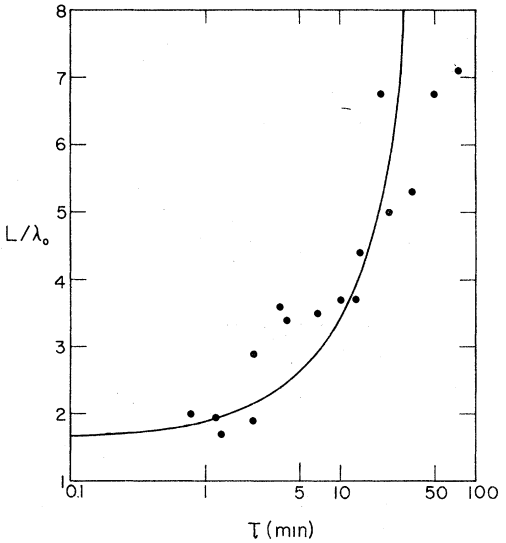

FIG. 10. Solid curve describes the best fit theoretical lifetime of the storage mode versus L/λ_0 using Eq. (5.1). Experimental points are due to Hulin (Ref. 9).

theory and experiment serves to provide a macroscopic check of the present theoretical description of the director field. A more direct and detailed spatial probe of the director field is called for, and, as suggested above, this could be achieved using optical techniques. We have also proposed a mechanism for the decay of the metastable storage mode as well as a simple phenomenological expression, Eq. (5.1), for the lifetime as a function of plate spacing. Unfortunately, a first-principles derivation of an expression for the lifetime is notoriously difficult and we have limited our theoretical treatment to choosing the free parameters so as to yield a best fit to Hulin's lifetime data.[9] The mechanism we have proposed for the decay of the storage mode is the creation, due to thermal fluctuations, of a small nematic region of critical size. This small nematic region rewinds in the stable Grandjean configuration and tirggers the same chain of events in the immediate environment. The reasonably good agreement between the theoretical and measured lifetimes argues for the plausibility of our proposed mechanism for the decay of the storage mode. However, a stronger theoretical foundation for this mechanism would be of great value.

ACKNOWLEDGMENTS

We are grateful to Dr. D. Mukamel for helpful remarks and to Professor M. Labes for a useful discussion.

APPENDIX A

Here we show that with a simple change of variables one can express all quantities of interest for the cholesteric storage mode, with $K_1=K_3\neq K_2$ in terms of the corresponding quantities for the case $K_1=K_2=K_3$. This transcription is well known for familiar cholesteric systems,[28] but we have reproduced it here for the storage mode in view of the more complicated circumstances, first, that the director depends on two spatial coordinates and, second, we are including a surface-free-energy term describing the interaction of the cholesteric and the confining plates.

We start with the Frank free-energy density for a left-handed cholesteric in the form

$$\mathcal{F}=\tfrac{1}{2}K_1(\nabla\cdot\vec{n})^2+\tfrac{1}{2}K_2(\vec{n}\cdot\nabla\times\vec{n}-q_0)^2 + \tfrac{1}{2}K_3(\vec{n}\times\nabla\times\vec{n})^2-\tfrac{1}{2}K_2q_0^2 . \tag{A1}$$

With $\vec{n}(\vec{r})=\hat{x}\sin\Phi(x,z)+\hat{y}\cos\Phi(x,z)$ and the choice $K_1=K_3\neq K_2$, Eq. (A1) reduces to the simplified form

$$\mathcal{F}=\frac{K_1}{2}\left(\frac{\partial\Phi}{\partial x}\right)^2+\frac{K_2}{2}\left(\frac{\partial\Phi}{\partial z}\right)^2-K_2q_0\frac{\partial\Phi}{\partial z} . \tag{A2}$$

If all three Frank constants are unequal, then a term $K_1\cos^2\Phi+K_3\sin^2\Phi$ replaces the coefficient K_1 multiplying $(\partial\Phi/\partial x)^2$ in (A2). If the cholesteric ordering is characterized by a pitch 2λ, i.e., $\Phi(x,z+\lambda)=\pi+\Phi(x,z)$, and if we include the surface-energy term described in the Introduction then the total free energy per unit volume is of the form

$$F=\frac{1}{2L\lambda}\int_{-L}^{L}dx\int_{-\lambda/2}^{\lambda/2}dz\left[\frac{K_1}{2}\left(\frac{\partial\Phi}{\partial x}\right)^2+\frac{K_2}{2}\left(\frac{\partial\Phi}{\partial z}\right)^2-K_2q_0\frac{\partial\Phi}{\partial z} + \tfrac{1}{2}C\Phi^2[\delta(x-L)+\delta(x+L)]\right] \tag{A3}$$

It is convenient to introduce a function $\phi(x,z)$, defined by

$$\Phi(x,z)=\pi(z/\lambda)+\phi(x,z) \tag{A4}$$

which is periodic in z with period λ. The Euler-Lagrange equation corresponding to Eq. (A3) is

$$K_1\frac{\partial^2\phi}{\partial x^2}+K_2\frac{\partial^2\phi}{\partial z^2}=0 \quad (-L<x<L) \tag{A5}$$

where ϕ satisfies the boundary condition

$$\mp K_1\frac{\partial\phi}{\partial x}(\pm L,z)-C\frac{\pi z}{\lambda}-C\phi(\pm L,z)=0 \quad (-\tfrac{1}{2}\lambda<z<\tfrac{1}{2}\lambda) \tag{A6}$$

Of course, if K_1 were equal to K_2 then Eq. (A5) would reduce to Laplace's equation and the problem defined by Eqs. (A3)–(A6) becomes identical to that considered in Ref. 12.

Now we define the quantities x', z', and λ' by the equations

$$x'=x,\ z'=(K_1/K_2)^{1/2}z,\ \lambda'=(K_1/K_2)^{1/2}\lambda . \tag{A7}$$

We also define a function $\phi'(x',z')$ by the relation

$$\phi(x,z)=\phi(x',(K_2/K_1)^{1/2}z')=\phi'(x',z') . \tag{A8}$$

Substituting Eqs. (A7) and (A8) in each of Eqs. (A3)–(A6), the resulting equations, expressed in terms of the primed variables, are precisely the basic equations of Ref. 12, for helical ordering with pitch $2\lambda'$, when K_2 becomes equal to $K_1=K_3$. That is, the director and free energy for helical ordering with pitch 2λ in the case $K_1=K_3\neq K_2$ are expressible in terms of the director and free energy of a system where K_2 is made equal to $K_1=K_3$ but having helical ordering with pitch $2\lambda'=2(K_1/K_2)^{1/2}\lambda$.

APPENDIX B

This appendix is devoted to deriving Eqs. (2.2) and (2.4) of the text. If the surface-energy coefficient C is infinitely large, the director angle, as given by Eq. (2.1) reduces to[29]

$$\Phi(x,z;\infty)=qz+\sum_{n=1}^{\infty}\frac{(-1)^n}{n}\frac{\cosh(2nqx)}{\cosh(2nqL)}\sin(2nqz)\,. \tag{B1}$$

If, further, we restrict our attention to cases where $L\geq\lambda$, then for all n we can replace $\cosh(2nqL)$ by $\frac{1}{2}e^{(2nqL)}$, and Eq. (B1) can be rewritten as

$$\Phi(x,z;\infty)=qz+A[2q(L-x),z]+A[2q(L+x),z]\,. \tag{B2}$$

The function $A(\mu,z)$ defined by

$$A(\mu,z)=\sum_{n=1}^{\infty}\frac{(-1)^n}{n}e^{-n\mu}\sin(2nqz)\quad(\mu\geq 0)\,, \tag{B3}$$

can readily be written in closed form. We have, successively,

$$\begin{aligned}A(\mu,z)&=\mathrm{Im}\sum_{n=1}^{\infty}\frac{(-1)^n}{n}\exp(-\mu+2iqz)n\\&=-\mathrm{Im}\ln(1+e^{-\mu+2iqz})\\&=-qz+\tan^{-1}[\tan(qz)\tanh(\tfrac{1}{2}\mu)]\,.\end{aligned} \tag{B4}$$

Substituting Eq. (B4) for the two A functions in Eq. (B2) yields Eq. (2.2) of the text.

If now C is finite but $L\geq\lambda$, referring to Eq. (2.1) of the text, we can again replace both $\cosh(2nqL)$ and $\sinh(2nqL)$ by $\frac{1}{2}e^{(2nqL)}$, and thus

$$\Phi(x,z;\mathfrak{C})\simeq qz+\mathfrak{C}\sum_{n=1}^{\infty}\frac{(-1)^n}{n(n+\mathfrak{C})}(e^{-2nq(L-x)}+e^{-2nq(L+x)})\times\sin(2nqz)\,. \tag{B5}$$

Using Eqs. (B2) and (B3) we can rewrite Eq. (B5) as

$$\Phi(x,z;\mathfrak{C})=\Phi(x,z;\infty)-\mathrm{Im}\sum_{n=1}^{\infty}\frac{(-1)^n}{n+\mathfrak{C}}[e^{-2nq(L-x-iz)}+(x\to -x)]\,. \tag{B6}$$

Now

$$\sum_{n=1}^{\infty}\frac{u^n}{n+\mathfrak{C}}=\frac{u}{1+\mathfrak{C}}F(1+\kappa,1;2+\kappa;u)\,, \tag{B7}$$

where

$$F(a,b;c;u)=1+\frac{ab}{1!c}u+\frac{a(a+1)b(b+1)}{2!c(c+1)}u^2+\cdots \tag{B8}$$

is the hypergeometric function. Using Eqs. (B2) and (B7) we can rewrite Eq. (B6) as

$$\Phi(x,z;\mathfrak{C})=\Phi(x,z;\infty)-\frac{1}{1+\mathfrak{C}}\mathrm{Im}[e^{-2q(L-x-iz)}F(1+\mathfrak{C},1;2+\mathfrak{C};-e^{-2q(L-x-iz)})+(x\to -x)]\,. \tag{B9}$$

For numerical purposes it is convenient to reexpress Eq. (B9) in terms of an integral. This is achieved using the integral representation[30]

$$F(a,b;c;u)=\frac{\Gamma(c)}{\Gamma(b)\Gamma(c-b)}\times\int_0^1 dt\,t^{b-1}(1-t)^{c-b-1}(1-tu)^{-a}\,, \tag{B10}$$

which applies for $\mathrm{Re}c>\mathrm{Re}b>0$. The final result takes the form

$$\Phi(x,z;\mathfrak{C})=\Phi(x,z;\infty)+\left(e^{-2q(L-x)}\sin 2qz\int_0^1 dt\,\frac{t^{\mathfrak{C}}}{1+2te^{-2q(L-x)}\cos 2qz+t^2e^{-4q(L-x)}}+(x\to -x)\right)\,. \tag{B11}$$

If $L\gtrsim 2\lambda$ one may drop the second term within the large parentheses in Eq. (B11) and Eq. (2.3) may be substituted for $\Phi(x,z;\infty)$. The final result for $\Phi(x,z;\mathfrak{C})$ is given by Eq. (2.4) of the text.

*This research was supported in part by a grant from the United States-Israel Binational Science Foundation (BSF) Jerusalem, Israel.

†A portion of the present work is described in the thesis of one of the authors (J.I.) submitted to Bar-Ilan University, in partial fulfillment of the requirements for the M.Sc. degree.

[1]G. H. Heilmeier and J. E. Goldmacher, Appl. Phys. Lett. 13, 132 (1968).

[2]J. E. Adams, W. Haas, and J. Wysocki, J. Chem. Phys. 50, 2458 (1969); Mol. Cryst. Liq. Cryst. 8, 9 (1969).

[3]W. Haas and J. E. Adams, Appl. Optics 7, 1203 (1969).

[4]W. Haas, J. Adams, and J. B. Flannery, Phys. Rev. Lett. 24, 577 (1970).

[5]F. J. Kahn, Phys. Rev. Lett. 24, 209 (1970).

[6]F. Rondelez and H. Arnould, CR Acad. Sci. B 273, 549 (1971).

[7]I. Rault and P. E. Cladis, Mol. Cryst. Liq. Cryst. 15, 1 (1971).

[8]F. Rondelez and J. P. Hulin, Solid State Commun. 10, 1009 (1972).

[9]J. P. Hulin, Appl. Phys. Lett. 21, 455 (1972).

[10]P. E. Cladis and M. Kléman, Mol. Cryst. Liq. Cryst.

16, 1 (1972).
[11]L. J. Yu and M. Labes, Mol. Cryst. Liq. Cryst. 28, 423 (1974).
[12]M. Luban, D. Mukamel, and S. Shtrikman, Phys. Rev. A 10, 360 (1974).
[13]This mode is variously referred to as the storage mode, focal conic texture, domain texture, and fingerprint texture. In this work, as well as previously in Ref. 12, we adopt the name "storage mode."
[14]In Ref. 12, the one-constant approximation $K_1=K_2=K_3$ $(=K)$ was adopted for the three Frank constants. Unless specified to the contrary, all formulas given below relate to this case. However, with the aid of a well known, simple change of variables one can also accommodate the case where $K_1=K_3\neq K_2$ (see Appendix A).
[15]These symmetry properties are derived directly from the complete Euler-Lagrange equation for $\hat{n}$, Eq. (3.3). For details see the M.Sc. thesis of one of the authors (J.I.) (Bar-Ilan University, 1975) (unpublished) Appendix I. In this thesis results are also given for the behavior of the storage mode in the presence of an external magnetic field.
[16]The data of Ref. 2 indicated that the pitch of the storage mode is the same as for the Grandjean mode. This can be attributed to the fact that the experiment was performed for the case of a free surface, rather than for a plates-cholesteric sandwich as we are considering.
[17]The result Eq. (2.3) for $\Phi(x,z;\infty)$ can also be derived directly by considering a semi-infinite cholesteric filling the half-space $t=L-|x|>0$. In the case of a planar director field $\hat{n}(x,t)=\hat{t}\sin F(s,t)+\hat{y}\cos F(s,t)$, with equal Frank constants, the angle $F(s,t)$ satisfies Laplace's equation $\nabla^2F(s,t)=0$ and, with $C=\infty$, is subject to the boundary conditions $F(0,t)=F(s,0)=0$, $F(\frac{1}{2}\lambda,t)=\frac{1}{2}\pi$, $F(s+\lambda,t)=\pi+F(s,t)$. It is sufficient to consider the restricted region of space $0<s<\frac{1}{2}\lambda$, $t>0$. Now we define a conformal mapping with the aid of the complex variables $\zeta=s+it$ and $\xi=u+iv=\sin^2(\pi\zeta/\lambda)$ so that the above specified region of space maps into the upper half of the ξ plane. Specifically, the boundary lines $s=0\,(t>0)$, $t=0\,(0<s<\frac{1}{2}\lambda)$, and $s=\lambda/2\,(t>0)$ map into the segments $(-\infty,0)$, $(0,1)$ and $(1,\infty)$ of the u axis, respectively. As such the problem reduces to the classic textbook problem of obtaining a solution of Laplace's equation, in the upper half of the ξ plane, which satisfies the prescribed boundary conditions along the u axis, $F(u,0)=0\,(u<1)$; $\frac{1}{2}\pi\,(u>1)$. Using the standard formula $F(u,v)=(v/\pi)\int_{-\infty}^{\infty}du'F(u',0)/[(u'-u)^2+v^2]$ and making the identification $s=z$, $t=L-|x|$, yields Eq. (2.3).
[18]P. G. de Gennes, *The Physics of Liquid Crystals* (Clarendon, Oxford, 1974), p. 199.
[19]R. B. Meyer, Solid State Commun. 12, 585 (1973).
[20]V. Vitek and M. Kléman, J. Phys. (Paris) 36, 59 (1975).
[21]The derivation of Eq. (2.8) closely parallels the analogous calculation for the free energy given in Appendix B of Ref. 12.
[22]This statement requires amendment for $z\simeq\pm\frac{1}{2}\lambda$. Referring to Eq. (2.1), one has $\Phi\to\pm\frac{1}{2}\pi$ for $z\to\pm\frac{1}{2}\lambda$. One can show that this same result obtains if one sums the *infinite* series in Eq. (2.8), but in general the error is substantial if one only sums the first few terms. However, for $z\neq\pm\frac{1}{2}\lambda$, the error made by summing the first n terms of Eq. (2.7), for any finite integer n, decreases rapidly to zero as $\lambda\to\infty$, i.e., if L is decreased towards the critical spacing L_c.
[23]See, for example, C. Williams, P. Pieránski, and P. E. Cladis, Phys. Rev. Lett. 29, 90 (1972).
[24]See Eq. (6.43) of Ref. 18.
[25]F. S. Acton, *Numerical Methods that Work* (Harper and Row, New York, 1970), pp. 483–485.
[26]Equation (4.2) is derived assuming that the dielectric-constant anisotropy $|\epsilon_{\parallel}-\epsilon_{\perp}|/\epsilon_{\parallel}\ll 1$. This condition is satisfied for the mesomorphic mixtures studied by Hulin (Ref. 9).
[27]In their experiments, Rondelez and Hulin (Ref. 8) and Hulin (Ref. 9) employed a series of differing values of λ_0. However, neither the data for $2R$ nor the lifetime τ show any systematic dependence on this parameter. As such we have adopted the value $2\lambda_0=16.5$ μm which coincides with an intermediate value of the pitch employed by Rondelez and Hulin.
[28]See, for example, P. G. de Gennes, C. R. Acad. Sci. B 266, 571 (1968).
[29]Equation (B1) coincides with Eq. (7) of Cladis and Kléman (Ref. 10), but the latter authors gave only an upper bound for the series, in contrast with our exact result, Eq. (2.2).
[30]M. Abramowitz and I. A. Stegun, *Handbook of Mathematical Functions* (National Bureau of Standards, Washington, D. C., 1964), Eq. 15.3.1.